



ELSEVIER

Available online at www.sciencedirect.com

SCIENCE @ DIRECT®

Continental Shelf Research 24 (2004) 1699–1715

CONTINENTAL SHELF
RESEARCH

www.elsevier.com/locate/csr

Floc fraction in the waters of the Po River prodelta

J.M. Fox^{a,*}, P.S. Hill^a, T.G. Milligan^b, A.S. Ogston^c, A. Boldrin^d

^a*Department of Oceanography, Dalhousie University, Halifax, NS, B3H 4J1, Canada*

^b*Fisheries and Oceans Canada, Bedford Institute of Oceanography, Dartmouth, NS, B2Y 4A2, Canada*

^c*School of Oceanography, University of Washington, Seattle, WA, 98195-7940, USA*

^d*Istituto di Scienze Marine—ISMAR, Biologia del Mare—C.N.R., Castello 1364/A, 30122 Venice, Italy*

Received 2 June 2003; received in revised form 5 April 2004; accepted 14 May 2004

Available online 19 August 2004

Abstract

Three independent methods of estimating the proportion of suspended material packaged within flocs, termed the floc fraction (f), were employed using hydrographic and suspended sediment data, and core and tripod-based observation data collected from the waters and sediments of the Po River prodelta throughout 2001. Using a floc size versus settling velocity relationship established in this study, floc fraction estimates were derived as follows: (1) by calculation of floc concentration in in situ images versus total suspended concentration using knowledge of floc effective density via Stokes' approximation; (2) by parameterization of disaggregated inorganic grain size (DIGS) distributions of bottom sediments to infer floc fraction in suspension necessary to produce the observed flux to the seabed; and (3) by calculating a mean representative floc fraction estimate for the system derived from estimates of floc bulk density. Calculated estimates of floc fraction are near unity at the river mouth, with the bulk of floc deposition occurring by the 8 m-isobath. Seaward and to the south of the river mouth, the suspension is not highly flocculated ($f \sim 0.08$). Subsequent transport and removal of deposited sediment from the prodelta, as suggested in previous study, is believed to occur within the bottom boundary layer.

© 2004 Elsevier Ltd. All rights reserved.

Keywords: Aggregation; Delta; Effective density; Floc; Floc fraction; Po River; Sedimentation; Settling velocity

1. Introduction

Fine particle marine aggregates, or flocs, are ubiquitous in the ocean (Shanks, 2002) and are considered responsible for the rapid flux of the majority of fine particles to the seabed (McCave,

1975; Drake, 1976; Shanks and Trent, 1980; Syvitski et al., 1995). Past studies of river sedimentation along continental shelves (Gibbs and Konwar, 1986; Boldrin et al., 1988; Kineke et al., 1991; Geyer et al., 2000) invoke flocculation as necessary and responsible for the observed sedimentation rates, yet the quantitative mass percentage of flocculated material in suspension, or floc fraction (f), in suspension remains poorly known.

*Corresponding author. Fax: +1-902-494-3877.

E-mail address: jfox@phys.ocean.dal.ca (J.M. Fox).

Knowledge of floc fraction is essential for accurate predictions of sedimentation, because deposition can change appreciably with even a small variation in floc fraction due to the substantial difference between floc and single grain settling velocities in river plumes (Hill et al., 2001). With a method to quantify floc fraction in suspension, a fuller understanding of the sedimentary dynamics of a given system would emerge. However, flocs are fragile, difficult to sample, and have physical properties yet to be fully resolved, complicating the task of estimating the floc fraction.

The goal of this paper is twofold: to apply three methods of floc fraction determination to the sedimentary dynamics of the Po River prodelta and to assess the validity of those methods. The method that has been applied previously in the literature uses Stokes' approximation for the settling rate of a sphere to calculate excess density based on floc size, which, in turn, provides the knowledge needed to calculate mass bound within flocs of a given size (Syvitski et al., 1995; Dyer and Manning, 1999; Curran et al., 2002a). Floc concentration can be calculated using size distributions of flocs from in situ images provided the total suspended sediment concentration is known. Estimates can also be achieved by examining sediment deposits. Parameterization of bottom sediment disaggregated inorganic grain size (DIGS) distributions allows estimates of the mass fraction of material deposited within flocs to be made (Kranck and Milligan, 1991; Kranck et al., 1996; Curran et al., 2004). In addition to these established methods, a new approach to floc fraction estimation based on the technique of Mikkelsen and Pejrup (2000) is applied. Using an in situ laser particle sizer, Mikkelsen and Pejrup (2000) calculated bulk density estimates of material in suspension, generating a bulk size versus bulk settling velocity relationship representing the field site as a whole. When this technique is applied to in situ photographs and corresponding concentration data, a mean representative estimation of floc fraction is possible. Essential to all these techniques is a size versus settling velocity relationship of flocs in the waters of the Po prodelta which can be applied directly to the Stokes' and bulk density methods, and from which a mean representative

floc settling velocity is applied to the DIGS method.

Following a large-scale flood of the Po River in October 2000, extensive coring, hydrodynamic profiling, including suspended sediment profiling of the receiving basin, and the deployment of a tripod for long-term observation of bottom boundary layer dynamics were undertaken as part of the Office of Naval Research EUROSTRATA-FORM program. Although abundant flocs were observed in the Po River and its prodelta environment (Fox et al., 2004), floc fraction could not be determined due to lack of a size versus settling velocity relationship in the system. Previous studies of floc settling suggest a similar settling rate (on the order of 1 mm s^{-1}) from regions of varied geographical and energetic conditions (McCave, 1975; Kranck et al., 1992; Fennessy et al., 1994; ten Brinke, 1994; Syvitski et al., 1995; Hill et al., 1998; Dyer and Manning, 1999; Sternberg et al., 1999). Determination of floc settling rates in a marginal sea such as the Northern Adriatic would be a welcome addition. By equipping the tripod with a settling column/video apparatus (Sternberg et al., 1996), all the elements necessary for estimation of floc fraction were available.

2. Methods

2.1. Overview

The Po River dominates sediment input to the Northern Adriatic Sea. Fed by the Alps to the north and west and by the Apennines to the south, the Po delivers an estimated 20 million tonnes of sediment annually (Nelson, 1970). In addition to natural inputs, the Po receives anthropogenic inputs from Italy's most industrialized regions. These large inputs allow the Po to influence the budgets of dissolved and particulate materials of the entire Adriatic sea (Matteucci and Frascari, 1997). The Po delta is a product of centuries of human manipulation and flow re-direction and today is the site of substantial sediment deposition and accumulation. The present-day delta has five major distributaries, with 60% of the flow passing

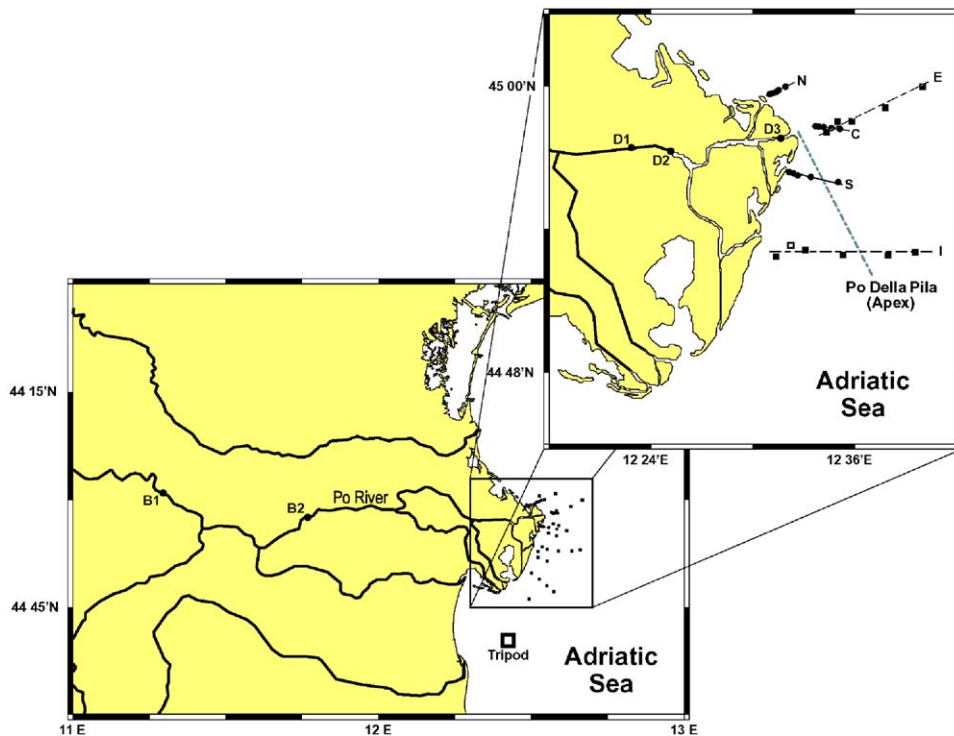


Fig. 1. Site Map of the study area. Station points are subdivided into those profiled from on board *Mysis* (circles) and *Sarom VIII* (squares). In the full domain view, every station from which a Bulk Settling Velocity estimate was made is marked as well as Bridge stations (B1, B2). In the magnified view, station transects are marked as North, Central, *E*-line, Southern, and *I*-line as well as Delta stations (D1–D3) from within the Po river. The tripod location (*T*) is marked with an open square.

through the Pila mouth located at the apex of the delta (Fig. 1).

Data collection was conducted in 2001 during cruises in January, June, and October. A tripod assembly was deployed January 25 and June 5 south of the delta at 14 m depth (Fig. 1), with retrieval occurring in June 5 and October 10, respectively. A settling column/video apparatus was affixed to the tripod at 2 m above the seabed, logging video of settling aggregates and collecting them in a trap at the base of the column (Sternberg et al., 1999). Box core samples were collected at the tripod location during each deployment and retrieval. Suspended sediment surveys took place in June and October involving collection of in situ suspended sediment photographs, water samples, transmissometer profiles, and surficial sediment samples as described in Fox et al. (2004). From June 4–7, a total of forty-four offshore stations

were profiled from the Istituto di Biologia del Mare–Consiglio Nazionale delle Ricerche (CNR-IBM) research vessel *Mysis* and the Micoperi vessel *Sarom VIII*. This investigation concentrated on five transects in the vicinity of the Pila mouth and the tripod location (Fig. 1). On October 14, two stations upstream of the mouth were visited for collection of in situ photographs and water samples. On October 16, three stations were profiled inside the delta with the addition of current meter readings from on board the *Mysis*. Disaggregated inorganic grain size (DIGS) distributions were measured with a Coulter Multi-sizer IIe for all core subsamples, settling column trap subsamples, surficial sediment samples, and suspended sediment samples with methods described previously (Milligan and Kranck, 1991).

Measurements were conducted over a relatively small range of environmental conditions.

Suspended particulate matter (SPM) was generally less than 15 mg l^{-1} , current speeds were generally less than 0.5 m s^{-1} , and the water column was highly stratified (Fox et al., 2004). As a result, turbulent kinetic energy dissipation rates, although unmeasured, were likely low. Because floc fraction depends on concentration as well as turbulent kinetic energy dissipation rate, floc fractions in turbid energetic environments likely would differ from those measured here.

2.2. Size versus settling velocity

The instrumentation of Sternberg et al. (1996, 1999) was used to collect size versus settling velocity data. The assembly consisted of a baffled settling trap with one transparent side, to which a Sony Hi8 Video Camera in a pressure housing was attached. Video was recorded for 10 s every 6 h over the course of each tripod deployment. The video was transferred to Sony DVcam tapes, generating a full digital data log of 720×480 pixel images with no signal loss. The camera used different powers of zoom for each deployment, resulting in a maximum resolution of 66 and $98 \mu\text{m}$ in January and June, respectively. Images from a resolvable burst of video were offloaded to a PC at intervals of 15 or 30 frames, depending on the speed of the settling flocs. A MATLAB script was executed to isolate the moving flocs in the image set, track the particle settling, and output independent estimates of diameter as equivalent spherical diameter (*ESD*), which considers the projected surface area of each floc to be circular, and elliptical nominal diameter (*END*), which considers projected surface area to be elliptical having a minor and major axis, and settling velocity (w_f). There were three periods where video proved to be unresolvable. On January 27, waves with a significant height of 4 m stirred the fluid in the settling column vigorously. On January 30, a downwelling-favorable Bora wind event generated enough resuspension to coat the transparent viewing surface and disabled particle detection for the remainder of the deployment. During the June deployment, sediment accumulation was sufficient to fill the trap, eliminating a working view by July 13.

2.3. In situ image analysis

At every station shown in Fig. 1, a Benthos 373 plankton silhouette camera cast was made through the water column in concert with other hydrographic instruments. Photographs were shot every 4 s. In situ suspended sediment photographs were analyzed as outlined in Fox et al. (2004). Prior to analysis, all photographs, having a depth of field of 4.0 cm, were duplicated using a Fuji FinePix S1 Pro digital SLR generating high resolution (3040×2016 pixel) grayscale image files. Binary thresholding, particle counting, and particle sizing were performed using Image Pro Plus (Media Cybernetics) PC image analysis software following the procedure of Curran et al. (2002b). The lower detection limit of particles within the images is $125 \mu\text{m}$, and as such, does not reflect a full complement of material in suspension. Median floc size (d_{50}) of each image was calculated as $\sqrt{(4/\pi)A_{50}}$, where A_{50} is the median floc area. Large particle volume concentration (LPVC) is the total volume of suspended material divided by the full volume represented in an image provided all the identified material is considered to be solid and spherical, with individual floc volumes a function of *ESD*. LPVC is expressed as parts per million and provides a representation of abundance of large particles in suspension (Milligan et al., 2001).

3. Determination of floc fraction

3.1. Stokes' approximation

Floc fraction estimates via Stokes' approximation have been made in previous studies (Syvitski et al., 1995; Dyer and Manning, 1999; Curran et al., 2002a). A fundamental assumption necessary to employ this method is to consider aggregates to exist in an environment where viscous forces of the surrounding fluid dominate the inertial forces of the aggregate. Calculation of Reynolds number (R_e) quantifies this relationship:

$$R_e = \frac{w_f d \rho}{\mu}, \quad (1)$$

where w_f is floc settling velocity (m s^{-1}), d is the aggregate diameter (m), ρ is the density of seawater (kg m^{-3}), and μ is dynamic viscosity ($\text{kg m}^{-1} \text{s}^{-1}$).

In a viscous regime ($Re \ll 1$), Stokes' approximation for a settling sphere can be rearranged to solve for effective density, $\Delta\rho$ (kg m^{-3}):

$$\Delta\rho = \frac{18\mu w_f}{gd^2}, \quad (2)$$

where g is gravitational acceleration (m s^{-2}).

Application of the size versus settling velocity data with corresponding viscosity data determined from temperature and salinity measurements, which we obtained from the tripod CTD, result in a size versus effective density relationship that can be applied to processed in situ still images to determine the mass bound within each floc image:

$$S_f = \frac{\Delta\rho}{\rho_s - \rho}, \quad (3)$$

$$M_f = \frac{\pi}{6} d^3 \rho_s S_f, \quad (4)$$

where S_f is the solid fraction of a given floc, ρ_s is the density of quartz (kg m^{-3}), and M_f is mass of a given floc (kg).

Each in situ image is representative of a volume of water. By dividing the sum of floc mass by the image volume, floc concentration is calculated. To complete determination of floc fraction, suspended particulate matter concentration at the depth of the image is necessary. This can be achieved by calibrating transmissometer data to known concentrations from water samples. The formal equation for floc fraction (f) is simply:

$$f = \frac{C_f}{SPM}, \quad (5)$$

where C_f is floc concentration (kg m^{-3}), and SPM is suspended particulate mass concentration (kg m^{-3}).

3.2. DIGS Parameterization

Consider that all material deposited on the seabed arrives as either single grains or flocs, and their relative proportions are representative of the

environmental conditions of deposition. This is the fundamental assumption behind the bottom sediment DIGS parameterization (Kranck et al., 1996; Milligan and Loring, 1997; Curran et al., 2004). If concentration of grain size class i ($C(i)$) is represented by the following equation:

$$C(i) = Q \left(\frac{d_i}{d_0} \right)^m e^{-(d_i/\hat{d})^2} \quad (6)$$

where d_0 is the reference diameter (m), Q represents the concentration of the reference diameter (kg m^{-3}), m represents the distribution of source material, d_i is the diameter of size class i (m), and \hat{d} is the diameter whose relative concentration is $1/e$ of its relative concentration in the source distribution (m), a non-linear fit of the size distribution is made to an equation for total flux:

$$J(i) = w_f f C(i) \left(1 + \left(\frac{d_i}{d_f} \right)^2 \right), \quad (7)$$

where $J(i)$ is the total flux of the i th size class to the seabed ($\text{kg m}^{-2} \text{s}^{-1}$) and d_f is the diameter at which the flux to the seabed is equal for single-grain and floc deposition. This parameter is termed the *floc limit* (m).

Estimates for m , \hat{d} , and d_f are made from the fit of Eq. (7) to a given distribution. To accommodate a proper fit, particle counts in the coarsest of size classes that reflect processes other than deposition from suspension (i.e. bedload) are excluded from the fit routine. These classes appear as a distinct mode or bulge in the coarsest part of the size distribution (Kranck and Milligan, 1991). The excluded points, however, are included in the integration calculation to obtain the fraction of mass deposited to the seabed within flocs (K_f):

$$K_f = \frac{\sum J(f)}{\sum J(t)}, \quad (8)$$

where $J(f)$ is flux bound within flocs and $J(t)$ is total flux. A graphical representation of the non-linear fit and parameters pertinent to this study can be found for a low and high K_f scenario in Fig. 2.

Now consider single-grain and floc flux written in terms of floc fraction:

$$J_s(i) = w_s(i)C(i)(1 - f), \tag{9}$$

$$J_f(i) = w_f C(i)f, \tag{10}$$

where $J_s(i)$ and $J_f(i)$ are single-grain and floc flux for the i th size class respectively ($\text{kg m}^{-2} \text{s}^{-1}$), $w_s(i)$ is the single-grain settling velocity of the i th size class (m s^{-1}), w_f is the mean floc settling velocity (m s^{-1}), $C(i)$ is the total concentration of the i th size class, and f is the floc fraction.

By solving for single-grain and floc flux of d_f , Eqs. (9) and (10) are set equal and rearranged to solve for f , that being the floc fraction necessary in suspension to generate the given flux:

$$f = \frac{\frac{w_s(d_f)}{w_f}}{1 + \frac{w_s(d_f)}{w_f}}. \tag{11}$$

Alternatively,

$$f = \frac{w_s(d_f)}{w_s(d_f) + w_f}. \tag{12}$$

A size versus settling velocity relationship is required to provide a mean representative floc settling velocity.

3.3. Bulk density estimates

Mikkelsen and Pejrup (2000) made bulk density calculations of material in suspension using volume concentration measurements from a LISST-100 in situ laser particle sizer paired with directly measured SPM values based on filtration of a 2 l water sample on 0.45 μm membrane filters:

$$\Delta\rho_b = \frac{SPM}{VC} \tag{13}$$

where $\Delta\rho_b$ is the bulk effective density of material in suspension (kg m^{-3}) and VC is the volume

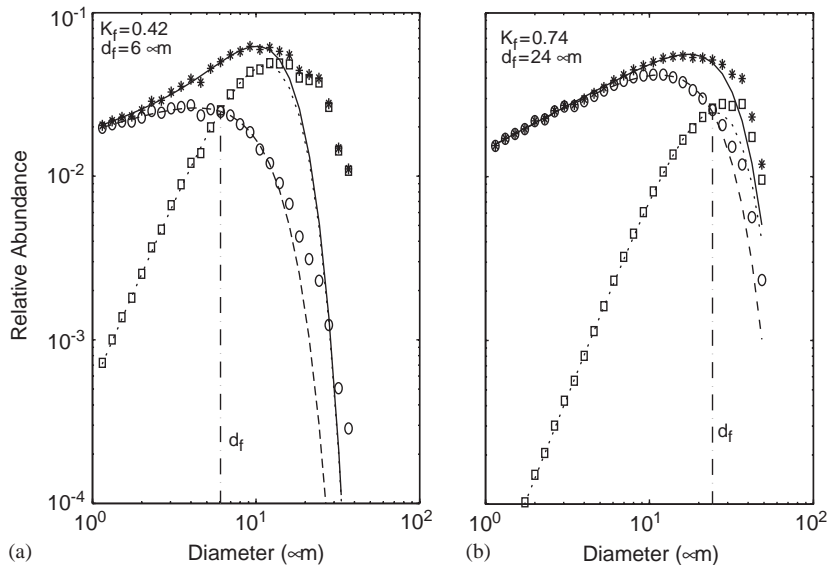


Fig. 2. Application of Disaggregated Inorganic Grain Size (DIGS) parameterization is displayed for selected 01/01-Trap (a) and 06/01-Core (b) sediment subsamples. The non-linear fit (solid line) of the full size distribution (asterisks) is fractionated into flux bound within flocs (circles and dashed line) and as single grains (squares and dotted line). Coarser material in the distribution is excluded from the fit routine as their arrival is from processes other than deposition from the water column. The area underneath the floc curve divided by the area under the total flux (asterisks) represents the fraction of material deposited to the seabed as flocs (K_f). The point of intersection of the floc and single-grain curves represents the diameter at which single-grain and floc fluxes are equal, termed the 'floc limit' (d_f). It is through the use of d_f that a calculation of the floc fraction in suspension necessary to generate the observed DIGS can be made.

concentration of material in suspension. The particle detection limit of the LISST-100 is 1.25–250 μm, allowing for the inclusion of fine single grain particles in suspension.

Given that volume concentration will be taken from still images as opposed to a laser sizer in our analysis, Δρ_b is re-defined in terms of SPM from a water sample and LPVC calculated from a collocated in situ image:

$$\Delta\rho_b = \frac{SPM}{LPVC} \tag{14}$$

Given a median size estimate from the size distribution, a bulk estimate of settling velocity can be calculated using Stokes' approximation and the median floc size *d*50 calculated from the same image for which LPVC was determined:

$$w_{sB} = \frac{g}{18\mu} \Delta\rho_b (d50)^2 \tag{15}$$

where *w*_{sB} is bulk settling velocity (m s⁻¹) and *d*50 is the median size of material in suspension (m).

The bulk size versus settling velocity relationship generated by this method assumes implicitly that all material in suspension is bound within the flocs visible in each image (*f* = 1). This relationship can then be compared to the established relationship from video analysis. The set of bulk estimates will overestimate floc settling rates as it is known that the images are not representative of the full suspended load. By that rationale, provided the slopes of the respective size versus settling velocity relationships are not significantly different, the offset of the intercept is directly proportional to the bulk density overestimate, and a floc fraction representative of the system as a whole can be determined. For example, if the bulk settling velocity relationship is 6× larger than the trend observed in the settling column, the floc fraction of the system would be *f* = 1/6 ~0.17.

4. Results

Resolvable video spanned January 26–29 and June 6–July 12, generating 209 and 200 estimates of floc size and settling velocity respectively. Regression analyses showed the 95% confidence

intervals of the respective data sets to overlap (Tables 1 and 2), allowing for a pooling of the data sets. The result is a data set of 409 independent estimates of size versus settling velocity (Fig. 3). Velocities ranged from 0.08 to 8 mm s⁻¹, with a mean settling velocity of 1.2 mm s⁻¹ based on number of flocs. For the smallest flocs analyzed, a pixelation effect is observed on a given image where arbitrary increases in floc size are represented by changes to a small number of pixels (< 4). By bin-averaging the data set into 1/3 Φ size classes, mean settling velocities emerge each associated with a logarithmic range of sizes, eliminating concerns about pixelation and serving to elucidate the relationship between mean size and settling velocity (Syvitski et al., 1995; Hill et al., 1998). Regression of the bin-averaged data provides expressions for settling velocity (m s⁻¹):

$$w_f = 86.95(ESD)^{1.33} \tag{16}$$

with *r*² = 0.97 where *ESD* indicates equivalent spherical diameter (m).

The same bin-averaging procedure was performed on the calculations of effective density (kg m⁻³):

$$\Delta\rho = 0.07(ESD)^{-0.76} \tag{17}$$

with *r*² = 0.88.

The results for equivalent spherical diameter and elliptical nominal diameter were closely

Table 1
Regression results: equivalent spherical diameter

Time period Data	<i>W</i> _s Expression (m s ⁻¹) <i>r</i> ²	Δρ Expression (kg m ⁻³) <i>r</i> ²
January	21.39(<i>ESD</i>) ^{1.22}	0.03(<i>ESD</i>) ^{-0.83}
Raw	0.57	0.37
January	81.19(<i>ESD</i>) ^{1.35}	0.12(<i>ESD</i>) ^{-0.70}
Bin Avg.	0.93	0.75
June	36.08(<i>ESD</i>) ^{1.24}	0.03(<i>ESD</i>) ^{-0.85}
Raw	0.55	0.36
June	31.79(<i>ESD</i>) ^{1.19}	0.06(<i>ESD</i>) ^{-0.81}
Bin Avg.	0.95	0.86
Jan + Jun	78.01(<i>ESD</i>) ^{1.35}	0.04(<i>ESD</i>) ^{-0.80}
Raw	0.63	0.38
Jan + Jun	86.95(<i>ESD</i>) ^{1.33}	0.07(<i>ESD</i>) ^{-0.76}
Bin Avg.	0.97	0.88

Table 2
Regression results: elliptical nominal diameter

Time period Data	W_s Expression (m s ⁻¹) r^2	$\Delta\rho$ Expression (kg m ⁻³) r^2
January	12.61(END) ^{1.16}	0.03(END) ^{-0.84}
Raw	0.56	0.39
January	35.37(END) ^{1.26}	0.14(END) ^{-0.69}
Bin Avg.	0.92	0.81
June	19.85(END) ^{1.17}	0.04(END) ^{-0.83}
Raw	0.54	0.38
June	38.95(END) ^{1.23}	0.06(END) ^{-0.80}
Bin Avg.	0.97	0.95
Jan + Jun	43.76(END) ^{1.29}	0.05(END) ^{-0.79}
Raw	0.61	0.40
Jan + Jun	77.60(END) ^{1.33}	0.10(END) ^{-0.74}
Bin Avg.	0.97	0.94

related (Tables 1 and 2) as a majority of the sample population was approximately spherical.

Application of Stokes' approximation to calculation of f for in situ images yields estimates greater than unity (Figs. 4–6). The largest floc fraction estimate ($f=2.92$) resides at 2.5 m at the 4 m station of the C-line directly offshore of the Pila mouth. Seaward and to the south of the 10 m station on the C-line, SPM and LPVC decrease considerably, with floc fractions remaining high ($f > 0.6$) throughout.

Parameterization of DIGS distributions at the tripod location provide floc fraction estimates in the range 0.04 to 0.10 (Table 3). The fraction of mass deposited to the seabed within flocs (K_f) was higher in the settling trap than in the seabed, yet

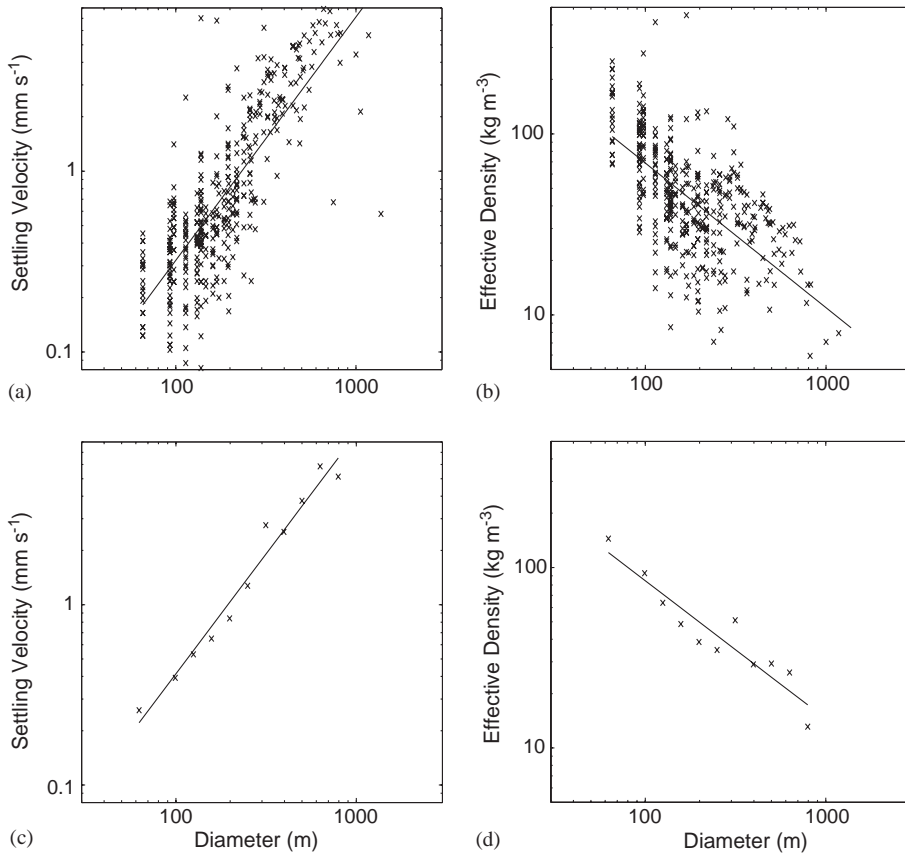


Fig. 3. The size (ESD) versus settling velocity relationship of Po prodelta flocs was obtained through video observation of 409 aggregates (a) in a settling column fixed to the tripod. Calculation of aggregate effective density was based on Stokes' Law (b). Bin-averaging of the data into $1/3\Phi$ size intervals was performed (c,d), yielding more robust relationships.

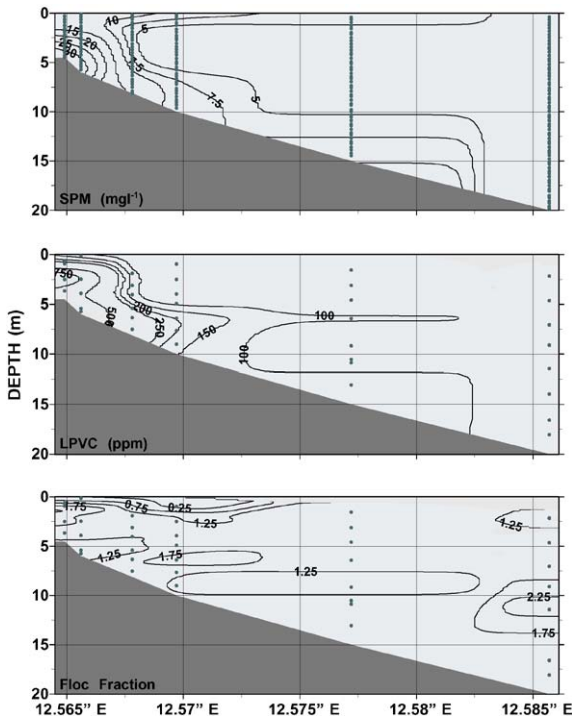


Fig. 4. Contours of suspended particulate matter (SPM), flocculation volume concentration (LPVC), and flocculation fraction (f) calculated via Stokes approximation are observed along the C-line off the mouth of the Pila mouth. Data points are marked in gray. SPM, LPVC, and flocculation fraction are highest at 2.5 m depth at the 4 m station, with all variables decreasing considerably by the 10 m station. Concentration increases at the 15 m-isobath, where bottom sediments likely become entrained in the southward drift current. Note that many flocculation fractions are well above unity, indicating that an assumption in the calculation is in error.

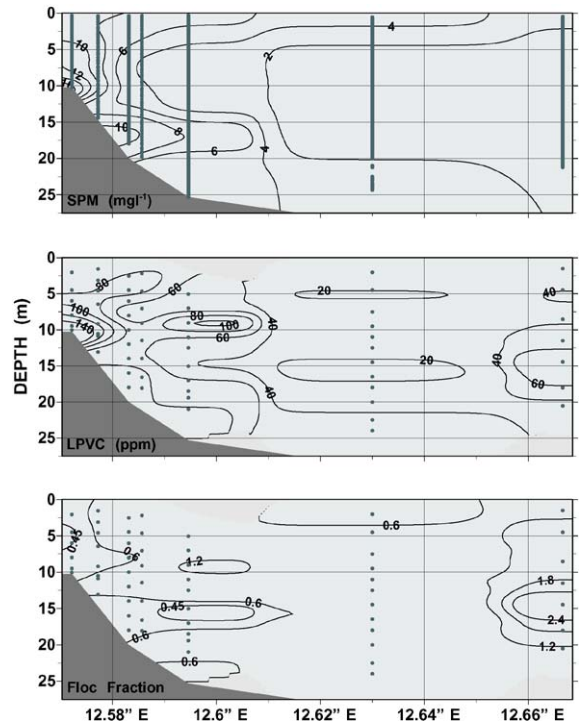


Fig. 5. Contours of suspended particulate matter (SPM), flocculation volume concentration (LPVC), and flocculation fraction (f) calculated via Stokes approximation are observed along the E-line off the mouth of the Pila mouth but in deeper water than the C-line. Sampling points are marked as gray dots. The highest concentrations are observed at the 10 m station and elevated concentration at the 15 m-isobath. Flocculation fractions are lower than observed on the C-line, suggesting that most material has been removed prior to the 10 m-isobath, beyond which bottom boundary layer transport is suggested to be responsible for the majority of sediment flux.

flocculation fraction was low and similar to that of the core sediments (Table 3). Surficial sediment DIGS parameters from the N, C, and S-lines indicate high flocculation fraction and a large proportion of flocculation deposition directly offshore of the Pila mouth between 6 m and 8 m ($f \sim 0.50$) with flocculation fraction decreasing ($f < 0.1$) seaward and to the south of the 10 m-isobath (Fig. 7). Elsewhere, high K_f values coupled with comparatively low f values reflect a suspension that is predominantly fine single grain particles. In such a suspension, low single grain settling velocities limit the single-grain flux to the seabed despite low flocculation fractions allowing for relatively high K_f values (Fig. 7).

The northern and southern transects both exhibit low flocculation fractions, with the northern transect receiving a greater proportion of flocculation-deposited material due to its proximity to a distributary channel to the North (Figs. 1 and 7). It is noteworthy that K_f values for the three transects converge at 15 m.

Sixty-three data points from 42 stations (Fig. 1) were available for bulk density estimates. The regression of bin-averaged bulk settling velocity estimates on bin-averaged diameters provides a slope ($m = 1.26$) close to that generated by settling video observation ($m = 1.33$). The intercept, however, is a factor of 4 larger for the bulk density

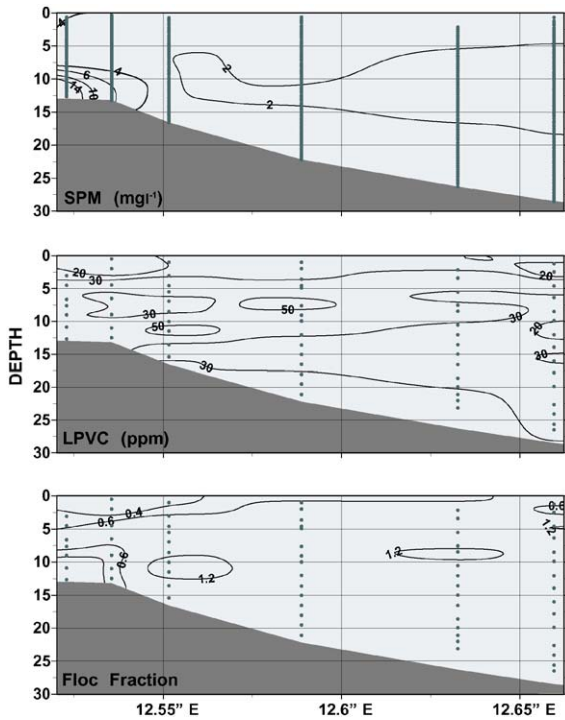


Fig. 6. Contours of suspended particulate matter (SPM), floc volume concentration (LPVC), and floc fraction (f) calculated via Stokes approximation are observed along the I-line in the vicinity of the tripod. Sampling points are marked as gray dots. Concentration is highest in shallow water near the seabed where floc fraction is also high. LPVC is low throughout the profile. As a result, floc fraction estimates beyond 12.5 m ($\text{SPM} < 4 \text{ mg l}^{-1}$) are prone to error.

Table 3
DIGS parameterization: tripod station

Sample	No. subsamples	Mean d_f (μm)	Mean K_f	Mean f
01/01-Core	9	8	0.31	0.04
01/01-Trap	8	10	0.52	0.07
06/01-Core-A	11	11	0.37	0.08
06/01-Core-B	12	11	0.43	0.09
06/01-Trap	18	12	0.62	0.09
10/01-Core	8	12	0.42	0.10

estimates than the direct observations of settling velocity, suggesting a bulk floc fraction estimate of 0.25 for the system as a whole (Fig. 8).

5. Discussion

The size versus settling velocity relationship obtained in this study resembles those from previous studies of size and settling from locations of varied energy and geography (Fig. 9) (McCave, 1975; Kranck et al., 1992; Fennessy et al., 1994; Syvitski et al., 1995; Sternberg et al., 1999). The slope of the trendline is slightly greater than those from studies in estuaries (Kranck et al., 1992; Fennessy et al., 1994; Syvitski et al., 1995), and slightly less than results from the exposed continental shelf (Sternberg et al., 1999) and the deep sea (McCave, 1975). The relationships established for the Po prodelta improve the precision of floc fraction determinations.

A wide range of floc fraction estimates emerge for the system from the three methods applied ($0.04 \leq f \leq 2.92$), will all overestimates associated with the Stokes' approximation method. Estimates that fall within a region of low SPM ($< 4 \text{ mg l}^{-1}$) and low LPVC ($< 50 \text{ ppm}$) are prone to error because they derive from the ratio of two small numbers, confining the focus here to waters landward of the 15 m-isobath (Figs. 4–6). When estimates are based on two parameters with low values, the range of results increases and the confidence is diminished. Aggregates observed in regions of low SPM and LPVC are primarily of large irregular and comet-like shapes, indicative of a high proportion of organic material which are not of relevance to the present study (Kranck and Milligan, 1991). The calibration of the transmissometer ($r^2 = 0.56$) was difficult to establish as a large range of turbidity readings existed for low concentration waters, likely reflecting variability in sediment size and composition (Baker and Lavelle, 1984) and the stronger bearing of aggregate size on suspended concentrations than on measured values of light attenuation (Mikkelsen and Pejrup, 2000). However, elimination of offshore data points still does not rectify the high floc fraction estimates made in the nearshore of the central transect where the conditions (SPM and LPVC) for estimation are considered most favorable and reliable (Fig. 4). Perhaps it is the assumptions necessary to apply Stokes' approximation which are problematic. For example, Li and Logan

(1997) showed that Stokes' Law underestimates settling velocities of aggregates. They attributed this result to reduced drag exerted due to channelling of fluid through pore spaces of the aggregate. The factor of underestimation ranges from 2.182 to 2.962 (Li and Logan, 1997). The

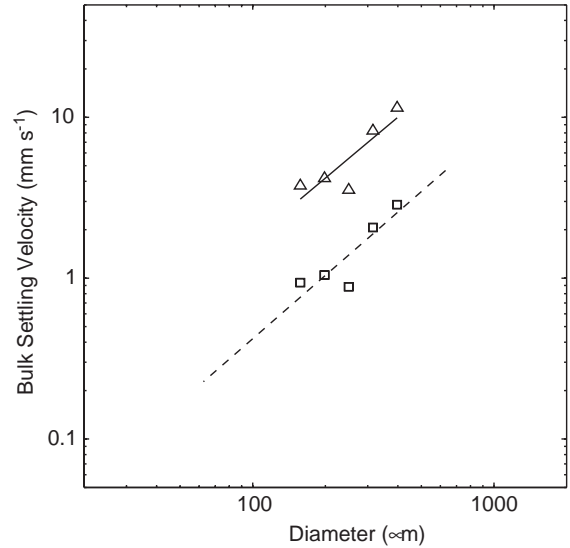
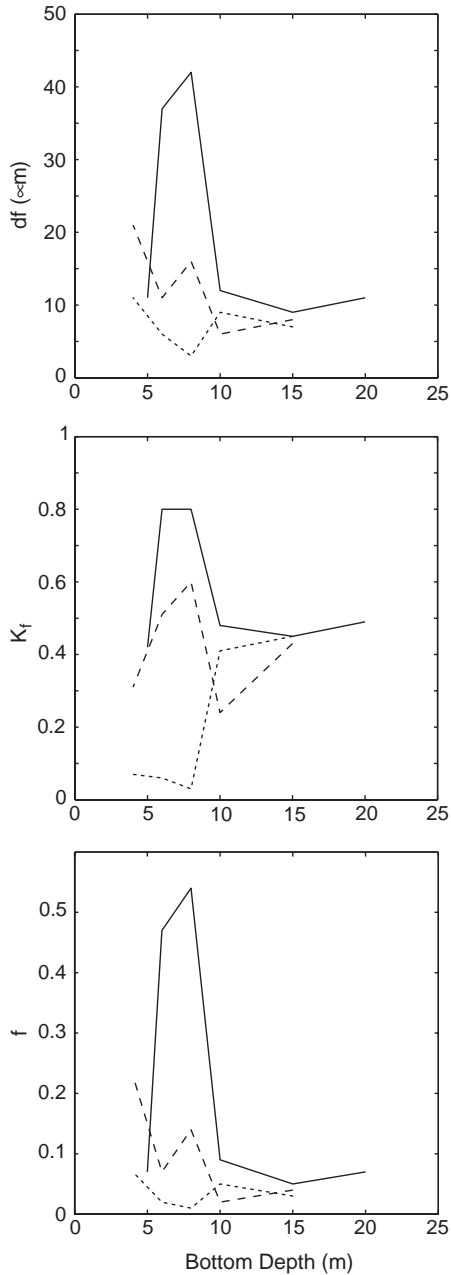


Fig. 8. Bin-averaged bulk settling velocity estimates are shown assuming all material visible in in situ photographs is bound within flocs ($f=1$) (triangles), and divided by an offset of 4 ($f=0.25$) (squares). The established size versus settling velocity relationship (dashed) shows the corrected bulk settling velocity estimates match the observed results.

location of highest abundance of flocs at 2.5 m depth at the 4 m C-line station (Fox et al., 2004) is the same location where the highest floc fraction estimate is reported ($f=2.92$). If it is assumed that floc fraction actually was unity at this location, floc density was overestimated by a factor of ~ 2.9 . By dividing all estimates of f by this factor, a more reasonable range of values results (Fig. 10). This correction factor lies within the range of Li and Logan (1997), and it provides values for f more

← Fig. 7. Profiles of floc limit (d_f), the fraction of mass deposited within flocs (K_f), and floc fraction (f) of surficial sediment samples are shown with depth along the N-line (dashed), C-line (solid), and S-line (dotted). The highest values of all three parameters occur along the C-line at depths of 6 and 8 m, where flocs deposit rapidly from suspension offshore of the river mouth. Along the N-line, intermediate K_f values are observed due to its proximity to a distributary channel to the north. The floc fractions along the N-line, however, are low. Along the S-line, K_f and f are extremely low in the nearshore, reflecting efficient removal of material in suspension along the C-line and the lack of a distributary channel in its vicinity. It is noteworthy that despite the contrasting dynamics of each transect, K_f values converge at 15 m where it has been suggested that bottom transport carries sediment southward.

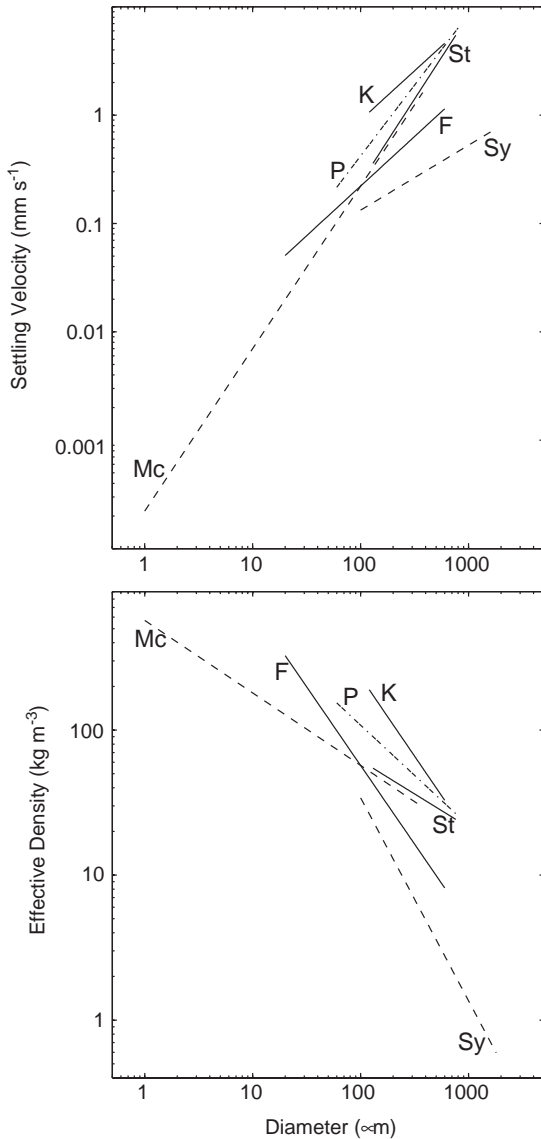


Fig. 9. The established size versus settling velocity relationship is compared to those determined from varied locations and energies. Studies are marked as follows: *Mc*=(*McCave*, 1975) from the Deep Sea, *K*=(*Kranck et al.*, 1992) from San Francisco Bay, *F*=(*Fennessy et al.*, 1994) from the Tamar Estuary, *Sy*=(*Syvitski et al.*, 1995) from Halifax Inlet, *St*=(*Sternberg et al.*, 1999) from the California Shelf, and *P*=present study. Excluding *Syvitski et al.* (1995), these studies show that on the average, flocs settle on the order of 1 mm s⁻¹, regardless of the sedimentary input and the dynamics of the system.

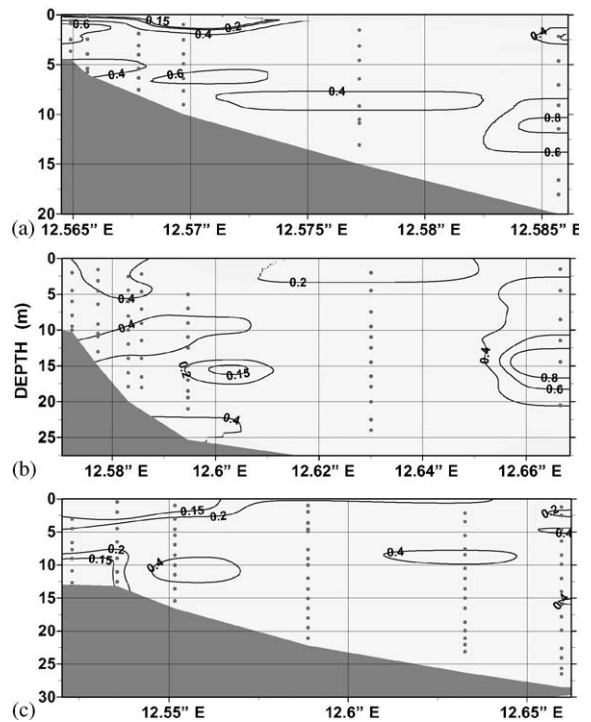


Fig. 10. Corrected *f* profiles for the C-line, E-line, and I-line: A correction factor of 2.9 is applied to the *f* profiles for the C-line (Top), E-line (Middle), and I-line (Bottom) following the results of *Li and Logan* (1997). Values are now within an acceptable range (*f*<1) with floc fraction dropping off immediately offshore of the river mouth (a,b), and low floc fractions to the south (c).

consistent with the DIGS results. Maximum floc fraction reported by the surficial sediment DIGS (~0.50) matches the corrected profile along the C-line (Fig. 10 top). Along the I-line at the tripod station, corrected Stokes' approximation floc fractions are between 0.15 and 0.2, which are higher than the core and trap DIGS estimates (*f* ~ 0.08). As the SPM and LPVC are relatively low at the tripod location, the I-line values may be overestimates.

The Stoke's Law underestimate of settling velocity (*Li and Logan*, 1997) also reflects an overestimate of effective density. Thus, the correction factor should also be applied to the bulk settling velocity estimates from the Mikkelsen/Pejrup method (*Mikkelsen and Pejrup*, 2000). By applying the correction factor used for Stokes

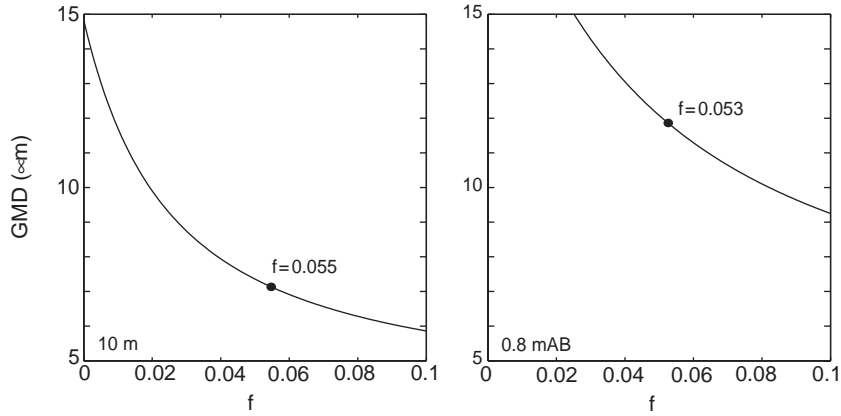


Fig. 11. From samples collected in June, Geometric Mean Diameters (GMD) of expected flux from the 10 m water sample above the settling trap and the 0.8 m AB water sample between the trap and bottom sediments are plotted as a function of flocculation fraction (solid line). The mean GMD determined from the trap and the core (filled circles) are plotted with the 10 m sample and 0.8 m AB sample, respectively. The flocculation fraction necessary to match the observed GMD in the deposited sediments is 0.055 (10 m) and 0.053 (0.8 m AB) showing that flocculation fraction remains the same even though the GMD increases from $\sim 7 \mu\text{m}$ to $\sim 12 \mu\text{m}$ as the suspension becomes increasingly more coarse closer to the seabed.

approximation estimates, the intercept of the settling velocity regression line based on bulk density is a factor of ~ 12 larger than the established relationship from direct observations. The corresponding flocculation fraction required to reconcile these two expressions is ~ 0.09 which is consistent with the DIGS estimates of f and broadly reconciles the results of the three estimation methods.

Flocculation fraction is high immediately seaward of the river mouth, where deposition occurs rapidly and removes the bulk of flocculated material from suspension by 8 m. A mid-water density interface impinges on the prodelta seafloor, serving to resuspend the deposited material and retain turbidity in the bottom boundary layer, where nearshore wave and current action are believed to transport material seaward along the bottom (Fox et al., 2004). A re-emergence of turbidity at 15 m is associated with a southward current which removes the material away from the prodelta (Fox et al., 2004). Seaward and to the south of the C-line, flocculation fractions are low, as are suspended concentrations and visible flocculation abundance (i.e.: LPVC) in the in situ images.

At the tripod station, the fraction of mass deposited to the seabed within flocs (K_f) is

higher in the sediment trap 2 m above the seabed than in the bottom sediments (Table 3). The trap sediments also have a higher mean d_f and overall lower proportion of coarser grains, yet values of f remain relatively consistent throughout (Table 3). If the suspension coarsens as the seabed is approached, K_f would be expected to decrease as the flux of coarser single grains to the seabed would rise while not necessarily altering the proportion of material bound within flocs in suspension. However, it has been suggested that as flocs approach the bottom boundary layer, shear stresses increase accordingly, initiating nearbed flocculation break-up (McCave, 1985; Hill et al., 2001). In an effort to establish the dominant cause of the difference between material settling to the trap versus the seabed, a simple calculation was performed using suspended size distributions from 3 m above the sediment trap (10 m) and in between the trap and the bottom sediments (0.8 m AB) collected in June. The flux to the seabed from each size class over a range of flocculation fractions can be calculated by summing Eqs. (9) and (10) to solve for total flux in size class i , $J(i)$:

$$J(i) = C(i)[w_s(i)(1 - f) + w_f f] \tag{18}$$

where w_f is the mean floc settling velocity (1.2 mm s^{-1}), and f is a pre-assigned floc fraction within the desired range which is being considered. The total flux is the sum over i of Eq. (18). Bottom sediment size distributions are calculated by dividing the flux in each size class by the total flux. Geometric mean diameter equals

$$GMD = 2 \left[-\sum_{i=1}^{n_{class}} \Phi(i) J(i) \right] \times 1000 \quad (19)$$

expressed in micron where $\Phi(i) = -\log d_{med}(i) / \log 2$ with $d_{med}(i)$ as the median diameter of size class i . GMD can be compared for various values of f .

Geometric mean diameter (GMD) of the 06/01-Trap and 06/01-Core DIGS distributions were calculated and compared to the GMD of the resultant synthetic flux distributions calculated with Eq. (18) for the 10 m and 0.8 m AB samples respectively (Fig. 11). The floc fraction for which the GMD from the deposited sediments and the synthetic flux GMD are equal is considered the floc fraction necessary in suspension to generate the observed deposit. Critical floc fractions are 0.055 and 0.053 for the waters above and below the trap respectively. Although a coarsening of the suspension occurs as the seabed is approached, the general uniformity of f in the DIGS parameterization results is supported, suggesting that resuspension, not floc break-up is responsible for the reduction of K_f at the tripod location as material approaches the seabed. The possibility that flocs are resuspended along with a coarse single grain population exists as previous observations suggest resuspended material from the Po prodelta to be highly flocculated (Matteucci and Frascari, 1997). Also, the minor increase in f at the tripod station from January to October might reflect the gradual removal of flood sediments from the prodelta. During flood events, the sediments would be generally coarser with more single-grain material exiting the river, reflecting deposition due to much greater energetic forcing than those at the time of sampling.

Fox et al. (2004) observed flocs far upstream of the river mouth in salinities of ~ 0.2 ppt. At the upstream bridge stations, in situ photographs and water samples were taken in the surface waters of

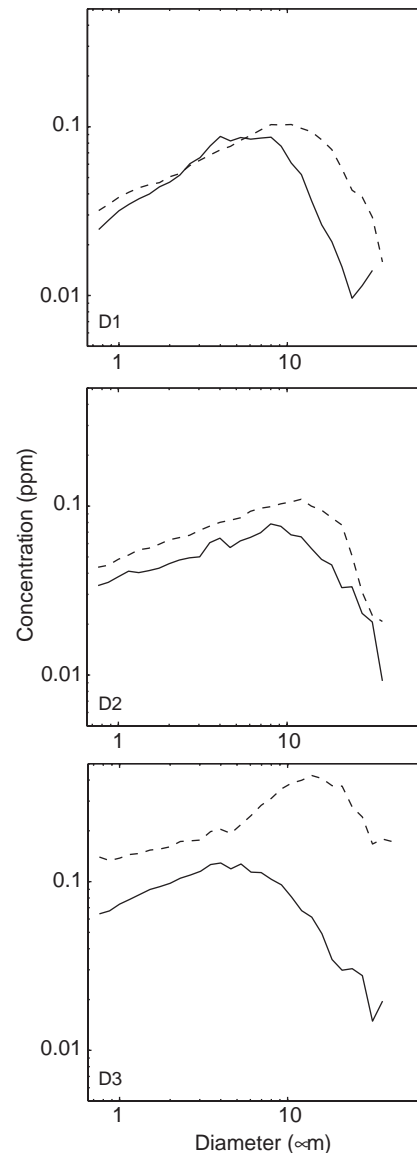


Fig. 12. Suspended DIGS distributions of surface water (solid lines) and 0.5 m AB water (dashed lines) samples are plotted for stations D1, D2, and D3 in the river. The water column is relatively well mixed at D1 and D2 as the two samples exhibit similar concentrations with the nearbottom sample having a naturally coarser end. At D3, concentration for both surface and bottom samples increase relative to D1 and D2 with the addition of a coarse mode to the nearbottom sample reflecting more extensive bottom resuspension.

the river. Corrected calculations of floc fraction were made with SPM values from the respective water samples, yielding floc fraction estimates of

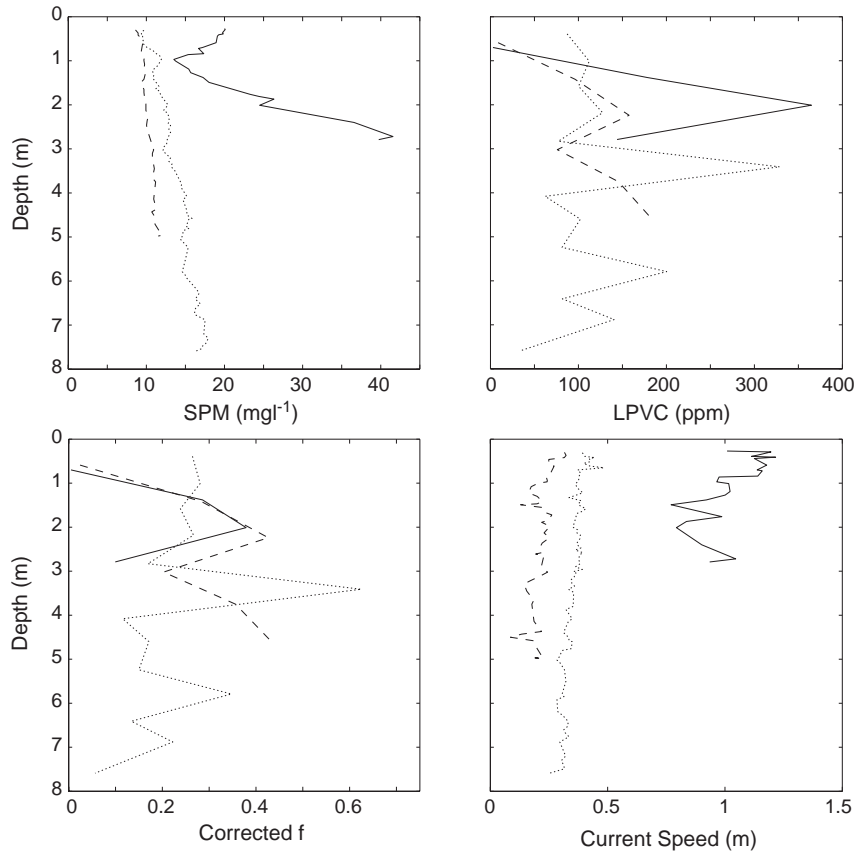


Fig. 13. Water column profiles of SPM (mg l^{-1}), LPVC (ppm), corrected f , and current speed (m s^{-1}) are plotted for stations D1 (dashed), D2 (dotted), and D3 (solid). As the river mouth is approached at D3, current speed increases twofold and SPM increases up to fourfold. Floc fraction at D3 has a maximum at ~ 2 m and decreases towards the seabed. Floc fraction at D2 and D3 show variation down column even though current magnitude and concentration are relatively constant.

0.51 and 0.55 for stations B1 and B2, respectively. At the stations within the delta, suspended size distributions show a water column that is well mixed at D1 and D2 as the surface and 0.5 m AB size distributions show a similar concentration and shape, with the near-bottom distribution having a naturally coarser end (Fig. 12). Where SPM and current speed are uniform through the column for D1 and D2, corrected floc fraction estimates are shown to fluctuate, with maximum values >0.40 (Fig. 13). As the flow is constricted through the more shallow waters at D3, current speed increases twofold and nearbed SPM increases fourfold, with LPVC and floc fraction decreasing nearbed (Fig. 13). The suspended DIGS at D3 show not

only an increase in concentration, but the near bottom sample is enriched with a modal resuspended single grain population from the seabed (Fig. 12), suggesting that the decrease in floc fraction is caused by bottom resuspension of coarse single grains and not by floc break-up. In comparison, if the difference between D3 and D2 DIGS distributions is examined ($dC(i) = C(i)_{D3} - C(i)_{D2}$), resuspension is further supported. Not only is the input of coarser single grains at D3 made clear, enrichment in fines is observed in the surface sample as the erosion and transport of smaller sized single grains from the seabed extend beyond that of progressively larger and heavier single grains (Fig. 14). The act of last-minute

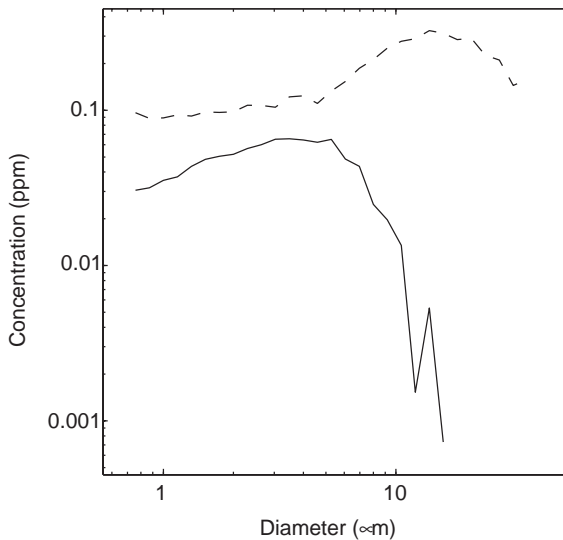


Fig. 14. The difference in DIGS distributions between D2 and D3 are plotted for the surface (solid line) and near-bottom (dashed line) water samples. The suspension at D3 is enriched in resuspended material relative to D2. The bottom sample receives resuspended input of all size classes including a coarse single-grain population seen in the modal distribution. The surface sample receives resuspended input void of coarse material as the liberation of fine grains from the seabed extends beyond that of increasingly coarser material.

mixing of a mature floc population with a resuspended single grain population, and the intruding salinity of the sea may further flocculate the suspension leading to the observed rapid removal. The mature flocs from far upstream appear to reach the nearshore prodelta intact, where floc sedimentation is rapid and nearly complete. Coarse single grains also sink rapidly to the seabed. The suspension remaining after initial deposition has a low degree of flocculation ($f \sim 0.08$) and is relatively fine-grained. During data collection periods, bottom boundary layer processes dominated sediment transport beyond the C-line.

By implementing the correction factor as per the findings of Li and Logan (1997), three methods for estimating floc fraction yield similar estimates in the waters of the Po prodelta. Future studies of floc dynamics would be enhanced by having collocated measurements of floc size, size versus settling velocity, DIGS, and sediment flux.

6. Conclusions

The goals of this study were to apply three methods of floc fraction determination and assess the validity of each method in interpreting the flocculation dynamics of the Po River prodelta system. Essential to all methods, the aggregate size versus settling velocity relationship was first determined ($w_f = 86.95 (ESD)^{1.33}$) on a sample set of 409 aggregates. The relationship, having floc settling velocities on the order of 1 mm s^{-1} , was consistent with results from studies in locations of varied geography and local energetics (Hill, 1998). With a correction factor in place to account for the effective density overestimate of Stokes' approximation, all three methods of floc fraction determination produce similar results. Flocs formed in the river deposit directly offshore of the river mouth, where the highest floc fraction of the system is observed ($f \sim 1$). The bulk of material is removed from the water column by the 8 m-isobath, where subsequent transport occurs within the bottom boundary layer. The remaining material in suspension is, for the most part, not highly flocculated ($f \sim 0.08$). A large improvement of such analyses would be to collocate all applicable instruments, making multiple localized studies simple and effective.

Acknowledgements

This study was supported by the U.S. Office of Naval Research contracts N00014-97-1-0160 and N00014-99-1-0113 and by EU project Eurodelta (Concerted Action n. EVK3-CT-2001-20001). Special thanks are given to ISMAR/BM and also to Ali Khelifa, for his thought-provoking input. Thanks are also given to Brent Law and Paul Macpherson in the Particle Dynamics Laboratory at the Bedford Institute of Oceanography for conducting particle size analysis. Preparation of the transect figures was carried out using Ocean Data View software designed by Reiner Schlitzer (<http://www.awi-bremerhaven.de/GEO/ODV2001>).

References

- Baker, E.T., Lavelle, J.W., 1984. The effect of particle size on the light attenuation coefficient of natural suspensions. *Journal of Geophysical Research* 89 (C5), 8197–8203.
- Boldrin, A., Bortoluzzi, G., Frascari, F., Guerizoni, S., Rabitti, S., 1988. Recent deposits and suspended sediments off the Po Della Pila (Po River, main mouth), Italy. *Marine Geology* 79, 159–170.
- Curran, K.J., Hill, P.S., Milligan, T.G., 2002a. Fine grained suspended sediment dynamics in the Eel River flood plume. *Continental Shelf Research* 22, 2537–2550.
- Curran, K.J., Hill, P.S., Milligan, T.G., 2002b. The role of particle aggregation in size-dependent deposition of drill mud. *Continental Shelf Research* 22 (3), 405–416.
- Curran, K.J., Hill, P.S., Schell, T.M., Milligan, T.G., Piper, D.J.W., 2004. Inferring the mass fraction of floc deposited mud: application to fine-grained turbidites. *Sedimentology*, in press.
- Drake, D.E., 1976. Suspended sediment transport and mud deposition on continental shelves. In: Stanley, D.J., Swift, D.J.P. (Eds.), *Marine Sediment Transport and Environmental Management*, Wiley, New York, pp. 127–158.
- Dyer, K.R., Manning, A.J., 1999. Observation of the size, settling velocity, and effective density of flocs, and their fractal dimensions. *Journal of Sea Research* 41, 87–95.
- Fennessy, M.J., Dyer, K.R., Huntley, D.A., 1994. Inseve: an instrument to measure the size and settling velocity of flocs in situ. *Marine Geology* 117, 107–117.
- Fox, J.M., Hill, P.S., Milligan, T.G., Boldrin, A., 2004. Flocculation and sedimentation on the Po River Delta. *Marine Geology* 203, 95–107.
- Geyer, W.R., Hill, P., Milligan, T., Traykovski, P., 2000. The structure of the Eel River plume during floods. *Continental Shelf Research* 20, 2067–2093.
- Gibbs, R.J., Konwar, L., 1986. Coagulation and settling of Amazon River suspended sediment. *Continental Shelf Research* 6 (1/2), 127–149.
- Hill, P.S., 1998. Controls on floc size in the sea. *Oceanography* 11 (2), 13–18.
- Hill, P.S., Syvitski, J.P., Cowan, E.A., Powell, R.D., 1998. In situ observations of floc settling velocities in Glacier Bay, Alaska. *Marine Geology* 145, 85–94.
- Hill, P.S., Voulgaris, G., Trowbridge, J.H., 2001. Controls on floc size in a continental shelf bottom boundary layer. *Journal of Geophysical Research* 106 (C5), 9543–9549.
- Kineke, G.C., Sternberg, R.W., Cacchione, D.A., Kranck, K., Drake, D.E., 1991. Distributions and characteristics of suspended sediment on the Amazon Shelf. *Oceanography Feature* (April), 21–26.
- Kranck, K., Milligan, T., 1991. Grain size in oceanography. In: Syvitski, J.P.M. (Ed.), *Principles Methods and Application of Particle Size Analysis*. Cambridge University Press, Cambridge, pp. 332–345.
- Kranck, K., Petticrew, E., Milligan, T.G., Droppo, I.G., 1992. In situ particle size distributions resulting from flocculation of suspended sediment. In: Mehta, A.J. (Ed.), *Nearshore and Estuarine Cohesive Sediment Transport*, Coastal and Estuarine Studies Series, Vol. 42. American Geophysical Union, Washington, pp. 60–75.
- Kranck, K., Smith, P.C., Milligan, T.G., 1996. Grain size characteristics of fine grained unflocculated sediments i: “one-round” distributions. *Sedimentology* 43 (3), 589–596.
- Li, X., Logan, B.E., 1997. Collision frequencies of fractal aggregates with small particles by differential settling. *Environmental Science and Technology* 31 (4), 1229–1236.
- Matteucci, G., Frascari, F., 1997. Fluxes of suspended materials in the North Adriatic Sea (Po Prodelt area). *Water, Air, and Soil Pollution* 99, 557–572.
- McCave, I.N., 1975. Vertical flux of particles in the ocean. *Deep-Sea Research* 22, 491–502.
- McCave, I.N., 1985. Mechanics of deposition of fine-grained sediments from nepheloid layers. *Geo-Marine Letters* 4, 243–245.
- Mikkelsen, O.A., Pejrup, M., 2000. In situ particle size spectra and density of particle aggregates in a dredging plume. *Marine Geology* 170, 443–459.
- Milligan, T.G., Kranck, K., 1991. Electro-resistance particle size analyzers. In: Syvitski, J.P.M. (Ed.), *Principles, Methods and Applications of Particle Size Analysis*. Cambridge University Press, New York, pp. 109–118.
- Milligan, T.G., Loring, D.H., 1997. The effect of flocculation on bottom sediment size distributions in coastal inlets and its implication for contaminant transport. *Water, Air and Soil Pollution*, 33–42.
- Milligan, T.G., Kineke, G., Blake, A., Alexander, C., Hill, P., 2001. Flocculation and sedimentation in the Ace Basin, South Carolina. *Estuaries* 24 (5), 734–744.
- Nelson, B.W., 1970. Hydrography, sediment dispersal, and recent historical development of the Po River Delta. In: Morgan, J.P. (Ed.), *Deltaic Sedimentation: Modern and Ancient*. Soc. Econ. Paleontologists and Mineralogists, New York, pp. 152–184.
- Shanks, A.L., 2002. The abundance, vertical flux, and still-water and apparent sinking rates of marine snow in a shallow coastal water column. *Continental Shelf Research* 22, 2045–2064.
- Shanks, A.L., Trent, J.D., 1980. Marine snow: sinking rates and potential role in vertical flux. *Deep-Sea Research* 27A, 137–143.
- Sternberg, R.W., Ogston, A., Johnson, R., 1996. A video system for in situ measurement of size and settling velocity of suspended particulates. *Journal of Sea Research* 36, 127–130.
- Sternberg, R.W., Berhane, I., Ogston, A.S., 1999. Measurement of size and settling velocity of suspended aggregates on the Northern California continental shelf. *Marine Geology* 154, 43–54.
- Syvitski, J.P.M., Asprey, K.W., Le Blanc, K.W.G., 1995. In situ characteristics of particles settling within a deep-water estuary. *Topical Studies in Oceanography* 42 (1), 223–256.
- ten Brinke, W.B.M., 1994. Settling velocities of mud aggregates in the Oosterschelde tidal basin (the Netherlands), determined by a submersible video system. *Estuarine Coastal and Shelf Science* 39, 549–564.